Evidence for Multiple Chiral Doublet Bands in ^{133}Ce

A. D. Ayangeakaa,[1] U. Garg,[1] M. D. Anthony,[1] S. Frauendorf,[1] J. T. Matta,[1] B. K. Nayak,[1,*] D. Patel,[1]
Q. B. Chen (陈启博),[2] S. Q. Zhang (张双全),[2] P. W. Zhao (赵鹏巍),[2] B. Qi (亓斌),[3] J. Meng (孟杰),[2,4,5]
R. V. F. Janssens,[6] M. P. Carpenter,[6] C. J. Chiara,[6,7] F. G. Kondev,[8] T. Lauritsen,[6] D. Seweryniak,[6] S. Zhu,[6]
S. S. Ghugre,[9] and R. Palit[10,11]

[1]*Department of Physics, University of Notre Dame, Notre Dame, Indiana 46556, USA*
[2]*State Key Laboratory of Nuclear Physics and Technology, School of Physics, Peking University, Beijing 100871, China*
[3]*School of Space Science and Physics, Shandong University at Weihai, Weihai 264209, China*
[4]*School of Physics and Nuclear Energy Engineering, Beihang University, Beijing 100191, China*
[5]*Department of Physics, University of Stellenbosch, Matieland 7602, Stellenbosch, South Africa*
[6]*Physics Division, Argonne National Laboratory, Argonne, Illinois 60439, USA*
[7]*Department of Chemistry and Biochemistry, University of Maryland, College Park, Maryland 20742, USA*
[8]*Nuclear Engineering Division, Argonne National Laboratory, Argonne, Illinois 60439, USA*
[9]*UGC-DAE Consortium for Science Research, Kolkata 700 098, India*
[10]*Tata Institute of Fundamental Research, Mumbai 400 005, India*
[11]*The Joint Institute for Nuclear Astrophysics, University of Notre Dame, Notre Dame, Indiana 46556, USA*

Two distinct sets of chiral-partner bands have been identified in the nucleus ^{133}Ce. They constitute a multiple chiral doublet, a phenomenon predicted by relativistic mean field (RMF) calculations and observed experimentally here for the first time. The properties of these chiral bands are in good agreement with results of calculations based on a combination of the constrained triaxial RMF theory and the particle-rotor model.

Described in terms of a coupling between deformation and orientation degrees of freedom, chirality represents a novel feature of triaxial nuclei rotating about an axis that lies outside the three planes spanned by the principal axes of its mean-field density distribution [1–5]. For a triaxial nucleus, the short, intermediate, and long principal axes form a screw with respect to the angular momentum vector, resulting in the formation of two chiral systems, with left- and right-handed orientations. The restoration of the broken chiral symmetry in the laboratory frame manifests itself as a pair of degenerate $\Delta I = 1$ bands with the same parity. Experimental evidence for such chiral band pairs has been found in the $A \sim 190$, $A \sim 130$, $A \sim 100$, and $A \sim 80$ mass regions of the nuclear chart [6–20].

Theoretically, chiral doublet bands have been successfully described by several formulations viz. the triaxial particle rotor model (TPRM) [1,21–23], the tilted axis cranking model with shell correction (SCTAC) [2,15,16], and Skyrme-Hartree-Fock [24,25] approaches, and the random phase approximation [26,27]. The general conditions for rotational chirality [1] imply that this phenomenon may appear for more than one configuration in the same nucleus. The resultant possibility of having multiple pairs of chiral doublet bands in a single nucleus was demonstrated for the Rh isotopes by the relativistic mean field (RMF) theory in Refs. [28–30], which introduced the acronym $M\chi D$ for multiple chiral doublet bands. The likelihood of chiral bands with different configurations was also discussed in context of SCTAC calculations used to interpret

the observed band structures in ^{105}Rh [15,16]. In this Letter, the first strong experimental evidence for the existence of $M\chi D$ is reported in the nucleus ^{133}Ce. The observations represent an important confirmation of triaxial shape coexistence and its geometrical interpretation.

Two separate experiments were performed using the ATLAS facility at the Argonne National Laboratory. In both, high-spin states in ^{133}Ce were populated following the ^{116}Cd(^{22}Ne, $5n$)^{133}Ce reaction at a bombarding energy of 112 MeV. In the first experiment, the target was a foil of isotopically enriched ^{116}Cd, 1.48 mg/cm^2 thick, and sandwiched between a 50 μg/cm^2 thick front layer of Al and a 150 μg/cm^2 thick Au backing. The second experiment used a target of the same enrichment and thickness evaporated onto a 55 μg/cm^2 thick Au foil. In both experiments, four-fold and higher prompt γ-ray coincidence events were measured using the Gammasphere array [31]. A combined total of approximately 4.1×10^9 four- and higher-fold coincidence events were accumulated during the two experiments. These events were analyzed using the RADWARE suite of analysis packages [32]. The level scheme for ^{133}Ce deduced in the present work builds substantially upon that previously reported for this nucleus [33–35]. A partial level scheme comprising the structures relevant to the focus of this Letter is displayed in Fig. 1. Spin and parity assignments for newly identified levels were made on the basis of extensive measurements of directional correlation of oriented nuclei (DCO) ratios [36,37] and, where practical, confirmed by angular-distribution analyses [38].

Two strongly coupled $\Delta I = 1$, positive-parity bands were established: the lower-energy band (band 2 in Fig. 1) and its partner (band 3) which feeds into the former by a number of strong $\Delta I = 1$, and much weaker $\Delta I = 2$, "linking" transitions. Both bands were known previously [33], but had no conclusive multipolarity and configuration assignments. They have been extended up to $I^\pi = \frac{33^+}{2}$ and new in-band crossover transitions have been added, together with the aforementioned linking transitions. From DCO ratios and angular-distribution analyses, the $\Delta I = 1$ transitions in bands 2 and 3 were found to be of the dipole or quadrupole type; they are assumed to be of $M1/E2$ mixed multipolarity. The corresponding crossover transitions within the bands were found to have $E2$ character. Likewise, the multipolarities of the $\Delta I = 1$, 328, 338, and 391 keV linking transitions were determined to be of the mixed $M1/E2$ type [39]. This, in conjunction with the deduced $E2$ multipolarity of the 544 and 615 keV transitions, establishes that bands 2 and 3 have the same parity. The observation of linking transitions between bands 2 and 3, and the hitherto unknown multiple decays of the two bands into band 1 via a series of $\Delta I = 1$ and $\Delta I = 2$ transitions, suggests an underlying similarity of

the quasiparticle configurations associated with these bands. These decay sequences are interpreted as possibly resulting from the interaction between bands 1 and 2 (and, by similar argument, bands 1 and 3), following detailed calculations based on triaxial RMF theory in which the configuration of band 1 was revised to $\pi[(1h_{11/2} \times (2d_{5/2})] \otimes \nu(h_{11/2})^{-1}$ from its previously assigned $\pi[(1g_{7/2})^{-1}(1h_{11/2})] \otimes \nu(h_{11/2})^{-1}$ configuration [33]. Consequently, bands 2 and 3 are assigned the $\pi[(1g_{7/2})^{-1}(1h_{11/2})] \otimes \nu(1h_{11/2})^{-1}$ configuration.

A second pair of composite bands, consisting of the sequences identified as bands 5 and 6 in Fig. 1, was also established, with both bands again comprising strong $\Delta I = 1$ and relatively weak $\Delta I = 2$ transitions. The inset in Fig. 1 displays summed spectra obtained using various gate combinations to highlight the in-band and interconnecting transitions in bands 5 and 6. The spins and parity of levels in band 5, which has been slightly extended by the addition of new transitions above the $45/2^-$ level, were suggested previously by Ma *et al.* [33]; these assignments have been confirmed by the present angular-distribution and DCO analyses. Band 6 is entirely new, and the $M1/E2$ nature of the in-band 363, 367, 442, 423, 468, and 491 keV
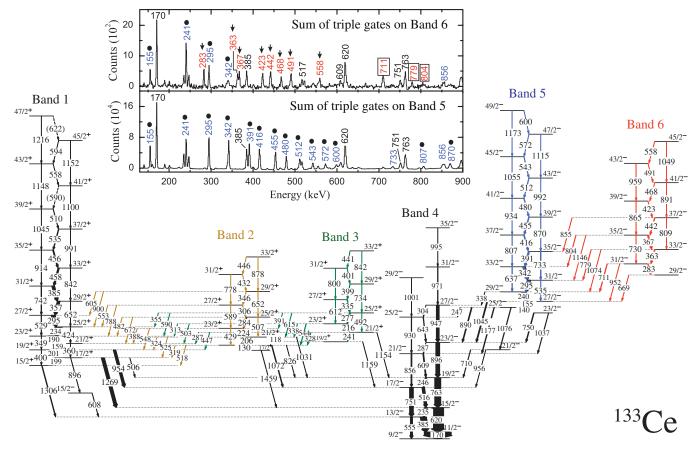

FIG. 1 (color online).   Partial level scheme of ^{133}Ce showing the previously known bands and the partner bands identified in this work. All transitions within and out a band are shown in the same color. The lowest level shown ($I^\pi = \frac{9^-}{2}$) is not the ground state, but an isomer with an excitation energy of 37.2 keV [46]. Inset: Background-subtracted γ-γ-γ-γ coincidence spectra from different gate combinations between bands 5 and 6. Black-, blue (with filled dots)-, and red (with arrows)-colored transitions represent members of bands 4, 5, and 6, respectively. The interconnecting transitions between bands 5 and 6 are identified by boxes around the transition energies.

transitions was deduced from the normalized ratios of γ-ray intensities in the detectors at forward angles to the intensities in the detectors at angles centered around 90°. This band forms a chiral pair with band 5 and decays into it via a number of strong $\Delta I = 1$ and some weak $\Delta I = 2$ transitions. The $M1/E2$ character of the 711 and 779 keV interconnecting transitions was again deduced from an angular-distribution analysis wherein the A_2/A_0 ratios were determined to be $-(0.622 \pm 0.013)$ and $-(0.7312 \pm 0.032)$, respectively. In addition, the DCO ratios for the 1074 and 1146 keV transitions were found to be consistent with a stretched-$E2$ character [39]. These results establish that band 6 has the same (negative) parity as band 5. Combined with the presence of strong interconnecting transitions, this observation also points to both bands having the same intrinsic configuration.

The standard fingerprints for chiral bands outlined in Ref. [40], i.e., close excitation energies, a constant staggering parameter, $S(I)$, and a similar behavior of the $B(M1)/B(E2)$ ratios, are evident for both chiral pairs in Fig. 2. Thus, there are *two* pairs of composite chiral partners, bands 2–3 and bands 5–6, in the same nucleus. This is the first instance of strong evidence for more than one set of chiral-partner bands in any nucleus. It should be pointed out that important confirmation of the chiral nature is provided by the measurement of transition probabilities in the two bands, as was clearly established in the case of the chiral bands in ^{135}Nd [26]. Although lifetime measurements were not feasible for bands reported here, the identical configuration of the chiral band pair in ^{135}Nd and

bands 5–6 in ^{133}Ce (see discussion below) provides further credence to these bands being chiral as well.

Calculations based on a combination of the constrained triaxial RMF theory [28–30] and the TPRM [22,23] have been performed to investigate the nature of the observed pairs of coupled bands and the presence of $M\chi D$ phenomenon in ^{133}Ce. The potential-energy surface in the β-γ plane for ^{133}Ce obtained from the RMF calculations with the parameter set PK1 [41] indicates that the calculated ground state of ^{133}Ce is triaxial ($\beta_2 = 0.20$, $\gamma = 11°$) and is soft with respect to the γ degree of freedom. By minimizing the energy with respect to the deformation γ, both the adiabatic and configuration-fixed β-constrained RMF calculations for ^{133}Ce have been performed for various low-lying particle-hole excitations; the results are provided in Fig. 3. The configuration, parity, deformation, and energy information for the calculated ground state (labeled A in Fig. 3), as well as for states "a" and "b" (regarded as bandheads of bands 2 and 5, respectively), are presented in Table I and compared with the experimental bandhead energies, and spins and parities I^π of the respective bands. The observed bandhead energies are reproduced reasonably well.

In order to examine the formation of chiral structures based on configurations a and b, the deformation parameters β and γ obtained from the RMF calculations were used as inputs to the TPRM calculations [23,42]. The moment of inertia of the rotor was adjusted to the experimental energies and the calculation of the electromagnetic transition probabilities followed the process described in Refs. [23,42].

The $\pi(1h_{11/2})^2 \otimes \nu(1h_{11/2})^{-1}$ quasiparticle configuration assigned to band 5 is due to the rotational alignment of a pair of $h_{11/2}$ protons coupled to an $h_{11/2}$ neutron hole after band crossing. A similar observation was made in Ref. [33], but the configuration of the band was suggested to be associated with a stable prolate axial ($\gamma = 0°$) shape.
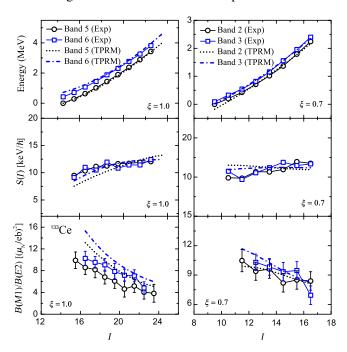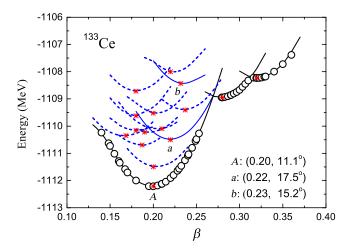

FIG. 2 (color online). Experimental excitation energies, $S(I)$ parameters, and $B(M1)/B(E2)$ ratios for the negative-parity chiral doublet (left panels) and positive-parity chiral doublet (right panels) in ^{133}Ce. Also shown are results of TPRM calculations with the indicated attenuation factors ξ (see text).

FIG. 3 (color online). Potential-energy curves in adiabatic (open circles) and various configuration-fixed β-constrained (solid and dashed curves) RMF calculations with the parameters set PK1 [41] for ^{133}Ce. The energy minima are represented as stars. The letters A, a, and b denote the calculated ground state, Band 2, and Band 5, respectively.

TABLE I.   The unpaired-nucleon configurations and parities for states A, a, and b, calculated with RMF. The deformation parameters β and γ, and the excitation energies E_x (in MeV) are provided, along with the experimental bandhead energies of Bands 2 and 5, based on the configurations a and b (see Fig. 3). The spin and parity I^π for bandheads of the two bands are also listed.

| | | | RMF calculations | | Experiment | | |
State	Unpaired nucleons	Parity	(β, γ)	E_x	Band	I^π	E_x
A	$\nu(1h_{11/2})^{-1}$	$-$	$(0.20, 11.1°)$	0.00			
a	$\pi[(1g_{7/2})^{-1}(1h_{11/2})^1] \otimes \nu(1h_{11/2})^{-1}$	$+$	$(0.22, 17.5°)$	1.71	band 2	$19/2^+$	2.378
b	$\pi(1h_{11/2})^2 \otimes \nu(1h_{11/2})^{-1}$	$-$	$(0.23, 15.2°)$	3.78	band 5	$29/2^-$	3.734

However, configuration assignments there were obtained with the assumption that the axis of rotation must coincide with one of the principal axes of the density distribution. In the present RMF calculations, the prolate minimum of the previous cranking calculations becomes a saddle point, and the actual minimum corresponds to a triaxial deformation capable of forming a chiral band.

TPRM calculations have been performed for band 5 and its proposed chiral partner, band 6, based on a $\pi(1h_{11/2})^2 \otimes \nu(1h_{11/2})^{-1}$ configuration and the results are presented in the left section of Fig. 2. The theoretical results show an impressive agreement with the data. The energy separation between the two bands is about 400 keV at $I = \frac{29}{2}$, and remains relatively constant over an extended spin range. Indeed, a similar band structure built on the $\pi(1h_{11/2})^2 \otimes \nu(1h_{11/2})^{-1}$ configuration was previously observed in ^{135}Nd and interpreted as a chiral composite structure [11,26]. The nucleus ^{133}Ce contains two fewer protons and the energy variation between bands 5 and 6 in Fig. 2 similarly suggests a form of chiral vibration, a tunneling between the left- and right-handed configurations, such that bands 5 and 6 are associated with the zero- and one-phonon state, respectively. Furthermore, the calculated staggering parameter $S(I)$ is seen to vary smoothly with spin (Fig. 2). This is expected since the Coriolis interaction is substantially reduced for a three-dimensional coupling of angular momentum vectors in a chiral geometry. A comparison of the calculated electromagnetic transition probability ratios with the data is presented in the lower panels of Fig. 2. In the TPRM calculations, no obvious odd-even staggering of the $B(M1)/B(E2)$ values is indicated, although a small effect is apparent experimentally. This further supports the interpretation in terms of a chiral vibration between bands 5 and 6 [43], which may be due to the softness of the triaxial shape [44].

The positive-parity chiral doublet bands built on the $19/2^+$ state (bands 2 and 3) are associated with the three-quasiparticle configuration $\pi[(1g_{7/2})^{-1}(1h_{11/2})^1] \otimes \nu(1h_{11/2})^{-1}$. The energy separation between bands 2 and 3 was found to be nearly constant at ~ 100 keV, which, combined with the spin-independent $S(I)$ parameter, leads to the interpretation of these bands being chiral partners as well. It should be noted that the two $M\chi D$ configurations in ^{133}Ce are analogous to the $\pi(1g_{9/2})^{-1} \otimes \nu[(1h_{11/2})^1(1g_{7/2})^1]$ and $\pi(1g_{9/2})^{-1} \otimes \nu(1h_{11/2})^2$ configurations proposed previously for ^{105}Rh [15,16].

The calculated excitation energies and the electromagnetic transition probability ratios $B(M1)/B(E2)$ for bands 2 and 3 are compared with the experimental values in the right panels of Fig. 2. It can be seen that the theoretical results are able to reproduce the data well: in the chiral region, the energy separation between bands 2 and 3 is nearly constant at ~ 100 keV, and the similar behavior of $B(M1)/B(E2)$ ratios is also clearly evident. Similar to bands 5 and 6, there is no perceptible staggering in the calculated $B(M1)/B(E2)$ ratios, but such an effect is apparent experimentally. The $B(M1)/B(E2)$ ratio depends sensitively on the details of the transition from the vibrational to the tunneling regime [23], which may account for the deviations of the TPRM calculation from experiment.

When comparing the experimental energies of bands 2 and 3 with the TPRM calculations, a Coriolis attenuation factor, $\xi = 0.7$, was employed. The incorporation of such an attenuation factor is not uncommon in the description of the properties of low-lying bands in deformed odd-A nuclei with TPRM [45] and might be a consequence of the fact that the configuration for these bands contains a low-j orbital $\pi(1g_{7/2})$ which has large admixtures with other low-j orbitals. The configuration for bands 5 and 6, on the other hand, contains only the high-j orbital $\pi(1h_{11/2})$, where the mixing is relatively small, thus alleviating the need for Coriolis attenuation.

In summary, two distinct chiral doublet bands based on the three-quasiparticle configurations $\pi[(1g_{7/2})^{-1} \times (1h_{11/2})^1] \otimes \nu(1h_{11/2})^{-1}$ and $\pi(1h_{11/2})^2 \otimes \nu(1h_{11/2})^{-1}$, respectively, have been observed for the first time in ^{133}Ce, and are interpreted in the context of the $M\chi D$ phenomenon. Calculations based on a novel combination of the RMF and TPRM reproduce the experimental results well, and confirm the manifestation of triaxial shape coexistence in this nucleus.

*Present address: Nuclear Physics Division, Bhabha Atomic Research Centre (BARC), Mumbai 400085, India.

[1] S. Frauendorf and J. Meng, Nucl. Phys. **A617**, 131 (1997).

[2] V. I. Dimitrov, S. Frauendorf, and F. Dönau, Phys. Rev. Lett. **84**, 5732 (2000).

[3] S. Frauendorf, Rev. Mod. Phys. **73**, 463 (2001).

[4] J. Meng and S. Q. Zhang, J. Phys. G **37**, 064025 (2010).

[5] J. Meng, Int. J. Mod. Phys. E **20**, 341 (2011).

[6] C. M. Petrache, D. Bazzacco, S. Lunardi, C. R. Alvarez, G. de Angelis, M. D. Poli, D. Bucurescu, C. Ur, P. B. Semmes, and R. Wyss, Nucl. Phys. **A597**, 106 (1996).

[7] K. Starosta, T. Koike, C. J. Chiara, D. B. Fossan, D. R. LaFosse, A. A. Hecht, C. W. Beausang, M. A. Caprio, J. R. Cooper, R. Krücken et al., Phys. Rev. Lett. **86**, 971 (2001).

[8] T. Koike, K. Starosta, C. J. Chiara, D. B. Fossan, and D. R. LaFosse, Phys. Rev. C **63**, 061304 (2001).

[9] A. A. Hecht, C. W. Beausang, K. E. Zyromski, D. L. Balabanski, C. J. Barton, M. A. Caprio, R. F. Casten, J. R. Cooper, D. J. Hartley, R. Krücken et al., Phys. Rev. C **63**, 051302 (2001).

[10] D. J. Hartley, L. L. Riedinger, M. A. Riley, D. L. Balabanski, F. G. Kondev, R. W. Laird, J. Pfohl, D. E. Archer, T. B. Brown, R. M. Clark et al., Phys. Rev. C **64**, 031304 (2001).

[11] S. Zhu, U. Garg, B. K. Nayak, S. S. Ghugre, N. S. Pattabiraman, D. B. Fossan, T. Koike, K. Starosta, C. Vaman, R. V. F. Janssens et al., Phys. Rev. Lett. **91**, 132501 (2003).

[12] T. Koike, K. Starosta, C. J. Chiara, D. B. Fossan, and D. R. LaFosse, Phys. Rev. C **67**, 044319 (2003).

[13] C. Vaman, D. B. Fossan, T. Koike, K. Starosta, I. Y. Lee, and A. O. Macchiavelli, Phys. Rev. Lett. **92**, 032501 (2004).

[14] P. Joshi, D. G. Jenkins, P. M. Raddon, A. J. Simons, R. Wadsworth, A. R. Wilkinson, D. B. Fossan, T. Koike, K. Starosta, C. Vaman et al., Phys. Lett. **595B**, 135 (2004).

[15] J. A. Alcántara-Núñez, J. R. B. Oliveira, E. W. Cybulska, N. H. Medina, M. N. Rao, R. V. Ribas, M. A. Rizzutto, W. A. Seale, F. Falla-Sotelo, K. T. Wiedemann et al., Phys. Rev. C **69**, 024317 (2004).

[16] J. Timár, P. Joshi, K. Starosta, V. I. Dimitrov, D. B. Fossan, J. Molnár, D. Sohler, R. Wadsworth, A. Algora, P. Bednarczyk et al., Phys. Lett. B **598**, 178 (2004).

[17] P. Joshi, M. P. Carpenter, D. B. Fossan, T. Koike, E. S. Paul, G. Rainovski, K. Starosta, C. Vaman, and R. Wadsworth, Phys. Rev. Lett. **98**, 102501 (2007).

[18] S. Y. Wang, B. Qi, L. Liu, S. Q. Zhang, H. Hua, X. Q. Li, Y. Y. Chen, L. H. Zhu, J. Meng, S. M. Wyngaardt et al., Phys. Lett. B **703**, 40 (2011).

[19] D. L. Balabanski, M. Danchev, D. J. Hartley, L. L. Riedinger, O. Zeidan, J.-y. Zhang, C. J. Barton, C. W. Beausang, M. A. Caprio, R. F. Casten et al., Phys. Rev. C **70**, 044305 (2004).

[20] E. Lawrie, P. A. Vymers, J. J. Lawrie, C. Vieu, R. A. Bark, R. Lindsay, C. J. Barton, G. K. Mabala, S. M. Maliage, P. L. Masiteng et al., Phys. Rev. C **78**, 021305(R) (2008).

[21] J. Peng, J. Meng, and S. Q. Zhang, Phys. Rev. C **68**, 044324 (2003).

[22] S. Q. Zhang, B. Qi, S. Y. Wang, and J. Meng, Phys. Rev. C **75**, 044307 (2007).

[23] B. Qi, S. Q. Zhang, J. Meng, S. Y. Wang, and S. Frauendorf, Phys. Lett. B **675**, 175 (2009).

[24] P. Olbratowski, J. Dobaczewski, J. Dudek, and W. Płóciennik, Phys. Rev. Lett. **93**, 052501 (2004).

[25] P. Olbratowski, J. Dobaczewski, and J. Dudek, Phys. Rev. C **73**, 054308 (2006).

[26] S. Mukhopadhyay, D. Almehed, U. Garg, S. Frauendorf, T. Li, P. V. M. Rao, X. Wang, S. S. Ghugre, M. P. Carpenter, S. Gros et al., Phys. Rev. Lett. **99**, 172501 (2007).

[27] D. Almehed, F. Dönau, and S. Frauendorf, Phys. Rev. C **83**, 054308 (2011).

[28] J. Meng, J. Peng, S. Q. Zhang, and S.-G. Zhou, Phys. Rev. C **73**, 037303 (2006).

[29] J. Peng, H. Sagawa, S. Q. Zhang, J. M. Yao, Y. Zhang, and J. Meng, Phys. Rev. C **77**, 024309 (2008).

[30] J. Li, S. Q. Zhang, and J. Meng, Phys. Rev. C **83**, 037301 (2011).

[31] I.-Y. Lee, Nucl. Phys. **A520**, c641 (1990).

[32] D. C. Radford, Nucl. Instrum. Methods Phys. Res., Sect. A **361**, 297 (1995).

[33] R. Ma, E. S. Paul, C. W. Beausang, S. Shi, N. Xu, and D. B. Fossan, Phys. Rev. C **36**, 2322 (1987).

[34] K. Hauschild, R. Wadsworth, R. M. Clark, P. Fallon, D. B. Fossan, I. M. Hibbert, A. O. Macchiavelli, P. J. Nolan, H. Schnare, A. T. Semple et al., Phys. Lett. B **353**, 438 (1995).

[35] K. Hauschild, R. Wadsworth, R. M. Clark, I. M. Hibbert, P. Fallon, A. O. Macchiavelli, D. B. Fossan, H. Schnare, I. Thorslund, P. J. Nolan et al., Phys. Rev. C **54**, 613 (1996).

[36] A. Krämer-Flecken, T. Morek, R. M. Lieder, W. Gast, G. Hebbinghaus, H. M. Jäger, and W. Urban, Nucl. Instrum. Methods Phys. Res., Sect. A **275**, 333 (1989).

[37] C. J. Chiara, M. Devlin, E. Ideguchi, D. R. LaFosse, F. Lerma, W. Reviol, S. K. Ryu, D. G. Sarantites, O. L. Pechenaya, C. Baktash et al., Phys. Rev. C **75**, 054305 (2007).

[38] V. Iacob and G. Duchene, Nucl. Instrum. Methods Phys. Res., Sect. A **399**, 57 (1997).

[39] A. D. Ayangeakaa, Ph.D. thesis, University of Notre Dame, 2013.

[40] K. Starosta, AIP Conf. Proc. **764**, 77 (2005).

[41] W. Long, J. Meng, N. Van Giai, and S. G. Zhou, Phys. Rev. C **69**, 034319 (2004).

[42] B. Qi, S. Q. Zhang, S. Y. Wang, J. Meng, and T. Koike, Phys. Rev. C **83**, 034303 (2011).

[43] B. Qi, S. Q. Zhang, S. Y. Wang, J. M. Yao, and J. Meng, Phys. Rev. C **79**, 041302 (2009).

[44] P. Joshi, M. P. Carpenter, D. B. Fossan, T. Koike, E. S. Paul, G. Rainovski, K. Starosta, C. Vaman, and R. Wadsworth, Phys. Rev. Lett. **98**, 102501 (2007).

[45] P. Ring and P. Schuck, The Nuclear Many-Body Problem (Springer, New York, 2004).

[46] Yu. Khazov, A. Rodionov, and F. G. Kondev, Nucl. Data Sheets **112**, 855 (2011).